

# Individual grain orientations and texture development of nanocrystalline electrodeposits showing abnormal grain growth

Uta Klement\*, Melina da Silva

Department of Materials and Manufacturing Technology, Chalmers University of Technology, SE-41296 Gothenburg, Sweden

Available online 29 September 2006

## Abstract

The electron backscatter diffraction (EBSD) technique has been used to determine grain orientations of abnormally grown grains in nanocrystalline Ni electrodeposits upon annealing. The results show that the first grown grains have a  $\langle 3\ 1\ 1 \rangle // \text{ND}$  orientation. Upon annealing further grain growth occurs and the preferred alignment of the abnormally growing grains changes from  $\langle 3\ 1\ 1 \rangle // \text{ND}$  to  $\langle 1\ 1\ 1 \rangle // \text{ND}$ . The subgrain coalescence model adopted from recrystallization is used to describe the occurrence of abnormal grain growth, and energy considerations are put forward for explaining the dominance of the  $\langle 1\ 1\ 1 \rangle // \text{ND}$  texture component after longer annealing treatments.

© 2006 Elsevier B.V. All rights reserved.

**Keywords:** Metals; Nanostructures; Crystal growth; Scanning and transmission electron microscopy; X-ray diffraction

## 1. Introduction

Technological application of nanocrystalline materials requires stability of the nanocrystalline microstructure at elevated temperatures which is often limited by grain growth. Common for most of the nanocrystalline electrodeposits investigated so far is the occurrence of abnormal grain growth upon annealing, that means the formation of a bimodal microstructure with grown grains in a still nanocrystalline microstructure [1–7]. Improving thermal stability in such nanocrystalline materials goes therefore hand in hand with circumventing the occurrence of abnormal grain growth.

It is however still not understood what makes certain grains grow at temperatures sometimes as low as 80 °C, but texture influences are discussed in this context [1,8]. Texture investigations can be performed by X-ray diffraction measurements, while individual grain orientations could so far only be obtained by tedious transmission electron microscopy (TEM) analysis [9]. Nowadays, microtexture investigations, i.e. analyses of local texture, are possible by use of the scanning electron microscopy (SEM) based electron backscatter diffraction (EBSD) technique. The advantage of EBSD over TEM is that a statistical significant amount of grains can be inspected within relatively short time. Furthermore, EBSD detectors are now sensitive enough

to routinely collect diffraction patterns at reduced acceleration voltages and low probe currents. The possibility to use a short working distance at the same time allows improving spatial resolution to about 10 nm [10].

Hence, the aim of this study is to apply EBSD techniques to investigate the orientations of abnormally grown grains upon annealing. The local orientation measurements (microtexture) are correlated to the macrotexture obtained by X-ray texture measurements.

## 2. Experimental

Electrodeposited nanocrystalline Ni was provided by Integran Technologies Inc., Toronto, Canada. Details about the electrodeposition technique can be found elsewhere [11]. The initial grain size is  $46 \pm 16$  nm as obtained from TEM dark field images and the total impurity content amounts to 400 ppm S and 160 ppm C, respectively, as measured by the Leco infrared absorption technique [2]. Annealing treatments were performed in a vacuum furnace for 15, 20 and 30 min at 250 °C.

Texture measurements were carried out by X-ray diffraction using a Siemens D-5000 Texture Goniometer (Cu K $\alpha$  radiation,  $\lambda = 0.15406$  nm) at the Institute of Structural Physics, Dresden University of Technology. (1 1 1), (2 0 0) and (2 2 0) pole figures were recorded.

EBSD measurements were performed in a LEO Supra 55VP at HKL Technologies A/S, Hobro, Denmark, equipped with an HKL Channel 5 EBSD system and a Nordlys II detector. Detailed description of the EBSD technique can be found elsewhere [9,10,12]. All samples were prepared by conventional polishing with diamond paste (7, 3 and 1  $\mu\text{m}$ ) followed by ion-polishing for 1 h (angle of incidence 2°).

For obtaining orientation maps (OM) an accelerating voltage of 12 kV, and a step size of 20 nm was used. As result of the small grain size, and due to

\* Corresponding author. Tel.: +46 31 772 1264; fax: +46 31 772 1313.  
E-mail address: uta.klement@chalmers.se (U. Klement).

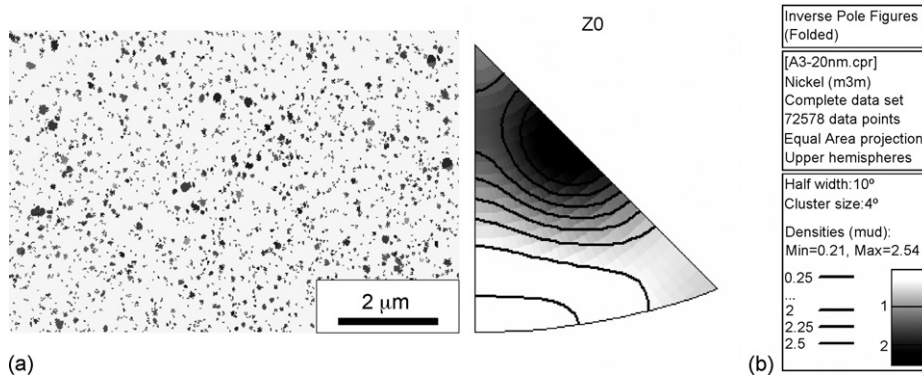


Fig. 1. (a) Orientation map (typical section) and (b) inverse pole figure of nanocrystalline Ni annealed at 250 °C for 15 min.

limitations in lateral and depth resolution of EBSD, the nanocrystalline matrix could not be analyzed. Grown grains formed during annealing could however be picked up and identified. Hence, the OM consist of unsolved pixels shown in white colour and indexed regions, i.e. grown grains, given in dark colour (grey shade). In all cases the same noise reduction was applied, i.e. wild spikes (single patterns) were removed and to some of the zero solutions a suitable orientation was assigned when the five nearest neighbours were equally indexed. Afterwards, grain identification was performed. Given grain diameters do not represent the real size of the grains, but relate to the area (amount of pixels) which is recognized as belonging to each grain (minimum two pixels). The measured textures are in general not very strong; intensities are at most three times random.

### 3. Results

After annealing for 15 min at 250 °C, a relatively large fraction of the investigated surface area could not be indexed. After noise reduction, the area fraction of the unindexed (white) region is 91%. Still, a few abnormally grown grains occur in the OM (Fig. 1a) with grain diameters ranging from 40 to 228 nm. For illustration of the alignment of the grains with respect to the sample normal (z-direction), inverse pole figures are used. As seen

in Fig. 1b, the first grown grains are preferentially of  $\langle 3\ 1\ 1 \rangle // ND$  oriented.

After annealing for 20 min at 250 °C, a higher fraction of the investigated surface area could be indexed, i.e. 19%, and grains with diameters of up to 441 nm are observed in the OM. For analyzing grain orientations in relation to grain size, the EBSD data was divided into subsets with the following grain size intervals: subset 1 = {40 nm, 100 nm}, subset 2 = {101 nm, 250 nm}, subset 3 = {251 nm, 441 nm}. The smallest grains are still  $\langle 3\ 1\ 1 \rangle // ND$  aligned while for the largest grains (subset 3) a double fiber texture with a weak  $\langle 3\ 1\ 1 \rangle // ND$  and a strong  $\langle 1\ 1\ 1 \rangle // ND$  component is observed.

After annealing for 30 min at 250 °C, the OM consists of grains with diameters up to  $\sim 1\ \mu\text{m}$  and the nanocrystalline matrix has basically disappeared (Fig. 2a). The unidentified area fraction after noise reduction amounts to 29% and is mainly due to defects like scratches on the sample surface and overlap of patterns at grain boundaries. Detailed investigation by use of grain size-subsets reveals that the smallest grains ( $\leq 100\ \text{nm}$ , Fig. 2b),

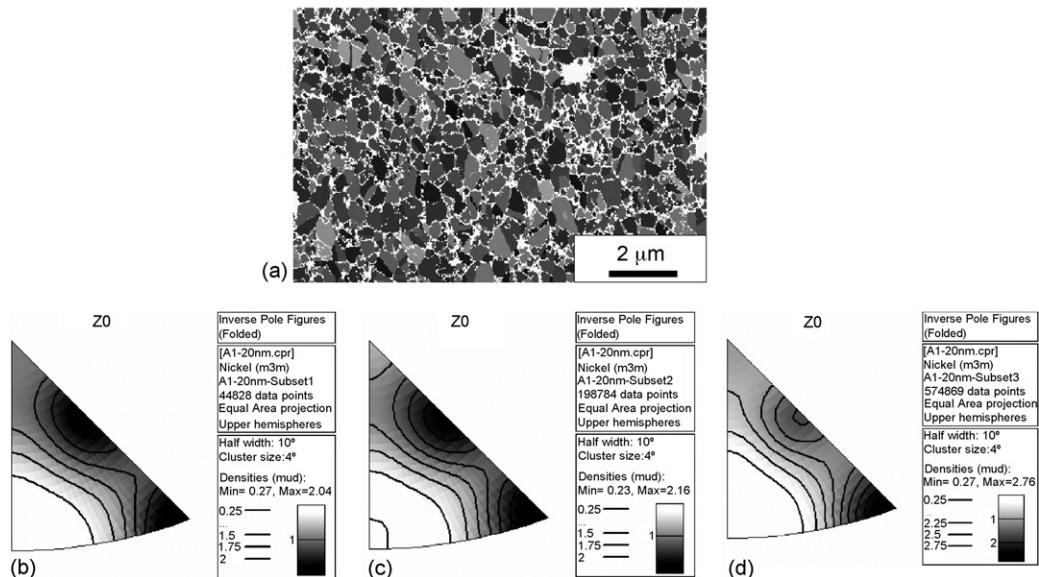


Fig. 2. (a) Orientation map of nanocrystalline Ni annealed at 250 °C for 30 min (typical section). (b–d) Inverse pole figures of Ni annealed for 30 min at 250 °C showing grain size subsets 1–3.

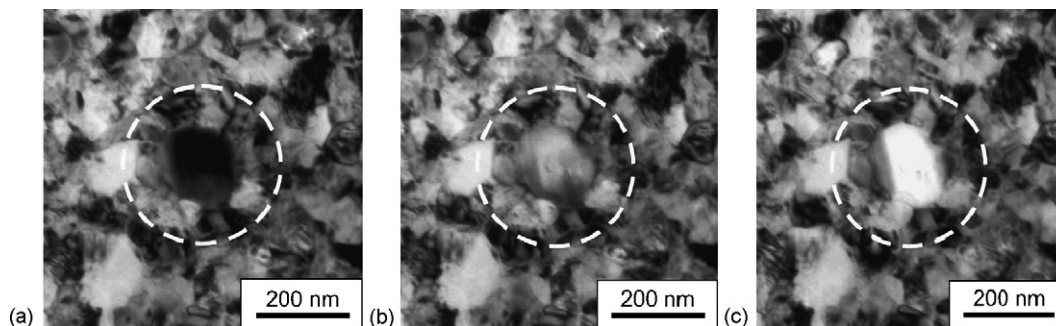


Fig. 3. (a–c) TEM-image sequence of growing grain during in situ annealing experiment.

making up 2% of the area fraction, show a  $\langle 3\ 1\ 1 \rangle // \text{ND}$  alignment. Grains with diameters between 100 and 250 nm (17% of the identified area fraction) show a double fiber texture consisting of a weak  $\langle 3\ 1\ 1 \rangle // \text{ND}$  and a strong  $\langle 1\ 1\ 1 \rangle // \text{ND}$  component (Fig. 2c), whereas grains larger than 250 nm are preferentially  $\langle 1\ 1\ 1 \rangle // \text{ND}$  oriented and dominate the OM with 52% of the identified area fraction (Fig. 2d). Moreover, for these large grains also an alignment in  $\langle 1\ 1\ 0 \rangle$ -direction is found in  $x$ - or  $y$ -axis (weak intensities in the respective inverse pole figures).

X-ray texture measurements on as-deposited Ni, and material annealed for 5 and 30 min at 250 °C in the differential scanning calorimeter (DSC) support the results obtained by EBSD analysis even though DSC annealing provides slightly different microstructures as compared to furnace annealing. As observed in TEM, the microstructures after 5 and 30 min annealing in the DSC correspond to 15 min and approximately 25 min furnace annealing, respectively. Already in the as-deposited material a double fiber texture is found with a weak  $\langle 1\ 1\ 1 \rangle // \text{ND}$  and a strong  $\langle 3\ 1\ 1 \rangle // \text{ND}$  component. After 5 min at 250 °C in the DSC, the  $\langle 3\ 1\ 1 \rangle // \text{ND}$  component is increasing slightly whereas after 30 min annealing, the  $\langle 3\ 1\ 1 \rangle // \text{ND}$  and  $\langle 1\ 1\ 1 \rangle // \text{ND}$  components are in principal equally strong.

#### 4. Discussion

Often, in an inhomogeneous grain size distribution the large grains are expected to grow primarily at the expense of the surrounding small grains. However, comparing the microstructural evolution upon annealing in electrodeposited nanocrystalline Ni with narrow and broad grain size distribution, larger grains were not found to grow first [2]. Furthermore, impurities cannot be held responsible for this behavior since the amount of C and S is three times higher in the material with narrow grain size distribution [2]. Additions of Fe, P and W have been proven to increase thermal stability of nanocrystalline Ni and Co electrodeposits substantially [2,13–16]. Such chemical influences may be the reason for the occurrence of abnormal grain growth if an inhomogeneous distribution of the solutes is assumed. Tomographic atom probe is probably the most suitable technique to provide detailed information about the solute content of grain boundaries upon annealing [17]. Unfortunately, the analyzed volume fraction is usually too small to allow conclusions regarding abnormal grain growth.

The importance of texture for the occurrence of abnormal grain growth has also been recognized. TEM observations of abnormally grown grains in nanocrystalline Ni could be explained by a subgrain coalescence model adopted from primary recrystallization [1]. In as-deposited Ni, grains of similar orientation can be found in close vicinity to each other, visible by their Moiré patterns. At elevated temperatures and as result of a relaxation process (achieving positions of lower energy) these grains are rotating slightly towards each other. Subgrain coalescence, which corresponds to removal of a low angle grain boundary, can then occur at these sites and first grown grains are formed. These grains are able to grow even further until ordinary grain growth takes place at sufficiently high temperatures [1].

In previous investigations of Ni and Ni-alloys, a  $\langle 2\ 0\ 0 \rangle \langle 1\ 1\ 1 \rangle$  double-fiber texture was found at the surface facing the substrate in the plating process [1,8,18–24]. Consistently, an increase of the  $\langle 1\ 1\ 1 \rangle // \text{ND}$  component at the expense of the  $\langle 2\ 0\ 0 \rangle // \text{ND}$  component was found upon annealing, i.e. when abnormal grain growth sets in. However, in none of the above-mentioned texture investigations (XRD and/or EBSD) the occurrence of a  $\langle 3\ 1\ 1 \rangle // \text{ND}$  component was observed. One possible explanation may be that in previous EBSD investigations much larger grains were analyzed and texture information was not obtained for different grain size intervals. Also, the broad grain size distribution and low solute content of the Ni electrodeposits investigated in this study may lead to a different texture as compared with materials having a more narrow grain size distribution. Regardless of the reason for the occurrence of  $\langle 3\ 1\ 1 \rangle // \text{ND}$ , the same arguments may apply for the preferred occurrence of the  $\langle 1\ 1\ 1 \rangle // \text{ND}$  after annealing.

Due to limitations in lateral and depth resolution of EBSD, it is not possible to analyze the misorientation between abnormally growing grains and surrounding nanocrystalline matrix. Hence, migration rates cannot be considered. X-ray texture analysis has however revealed that the as-deposited material has a double fiber texture in which  $\langle 3\ 1\ 1 \rangle // \text{ND}$  is stronger than  $\langle 1\ 1\ 1 \rangle // \text{ND}$ . The presence of a number of small angle grain boundaries between neighbouring grains with similar orientation supports earlier assumption that a process similar to subgrain coalescence is responsible for formation of first abnormally growing grains. Why  $\langle 1\ 1\ 1 \rangle // \text{ND}$  oriented grains are dominating the later texture instead of  $\langle 3\ 1\ 1 \rangle // \text{ND}$  grains, is determined by the presence of

solutes and second phase particles as well as by energy considerations.

According to computer simulations by Li et al. [25] for Ni–20% Fe, the surface energy is lowest for  $\{111\}$  planes and increases in the order of  $\{100\}$ ,  $\{110\}$ ,  $\{311\}$ ,  $\{210\}$ , etc. Hence, a strong  $\langle 111 \rangle$ //ND texture is expected to develop due to energy minimization. At elevated temperatures, each site may continually change position and orientation by diffusion and rotation to decrease the total energy of the system. During in situ annealing experiments in the TEM, distinct changes in the grey shade of growing grains have been observed (Fig. 3a–c). That suggests that Bragg condition, i.e. the grain orientation, has changed for the respective grain. Even though the observations are lacking support by diffraction measurements, there may be a relation to the process described above. Comparison with EBSD results reveals that the  $\langle 111 \rangle$ //ND component increases in importance for grain sizes  $>200$  nm. First results from EBSD investigations in Ni–20% Fe are pointing in the same direction (similar texture components and behavior upon annealing).

Seo et al. [8] support the argument of minimization of total energy. They have found a difference in volumetric energy between  $\langle 111 \rangle$ //ND and  $\langle 200 \rangle$ //ND grains by comparing interatomic distances for the  $\{111\}$  and  $\{200\}$  peaks in Ni and Ni-Fe (calculated from synchrotron XRD peaks) before and after annealing. Already in as-deposited state,  $\langle 111 \rangle$ //ND grains are expected to be in (or close to) equilibrium whereas  $\langle 200 \rangle$ //ND grains are deviating from their stable position [24]. Following that argumentation, abnormal grain growth can be interpreted by means of the orientation dependence of energy density in as-deposited state. The  $\langle 111 \rangle$ //ND grains having the lowest energy density (about 1 J/mol lower than for  $\langle 200 \rangle$ //ND as determined by Park et al. [23]) may grow into differently oriented grains to reduce total energy of the system.

## Acknowledgements

Thanks to Dr. P. Trimby, HKL Technologies A/S, for performing the EBSD measurements with the Nodlys II detector and to Prof. W. Skrotzki, Technical University Dresden, for assisting with XRD measurements on the nanocrystalline electrodeposits.

## References

- [1] U. Klement, U. Erb, A.M. El-Sherik, K.T. Aust, *Mater. Sci. Eng. A* 203 (1995) 177–186.
- [2] M. da Silva, U. Klement, *Z. Metallkd.* 96 (2005) 1009–1014.
- [3] G. Hibbard, U. Erb, K.T. Aust, U. Klement, G. Palumbo, *Mater. Sci. Forum* 386–388 (2002) 387–396.
- [4] M. Thuvander, M. Abraham, A. Cerezo, G.D.W. Smith, *Mater. Sci. Technol.* 17 (2001) 961–970.
- [5] P. Choi, M. da Silva, U. Klement, T. Al-Kassab, R. Kirchheim, *Acta Mater.* 54 (2005) 4473–4481.
- [6] B. Günther, A. Kumpmann, H.D. Kunze, *Scripta Metal. Mater.* 27 (1992) 833–838.
- [7] V.Y. Gertsman, R. Birringer, *Scripta Metal. Mater.* 30 (1994) 577–581.
- [8] J.H. Seo, J.K. Kim, Y.B. Park, in: L.L. Shaw, C. Suryanarayana, R.S. Mishra (Eds.), *Processing and Properties of Structural Nanomaterials*, The Minerals, Metals & Materials Society, 2003, pp. 213–218.
- [9] V. Randle, O. Engler, *Introduction to Texture Analysis, Macrotexture and Orientation Mapping*, Gordon, and Breach Science Publishers, Amsterdam, 2000.
- [10] <http://www.hkltechnology.com>.
- [11] U. Erb, A.M. El-Sherik, US Patent 5,352,266 (1994).
- [12] A. Schwartz, M. Kumar, B. Adams, *Electron Backscatter Diffraction in Materials Science*, Kluwer/Plenum, New York, 2000.
- [13] K. Boylan, D. Ostrander, U. Erb, G. Palumbo, K.T. Aust, *Scripta Metal. Mater.* 25 (1991) 2711–2716.
- [14] D. Osmola, P. Nolan, U. Erb, G. Palumbo, K.T. Aust, *Phys. Status Solidi A* 131 (1992) 569–575.
- [15] S.C. Mehta, D.A. Smith, U. Erb, *Mater. Sci. Eng. A* 204 (1995) 227–232.
- [16] P. Choi, T. Al-Kassab, F. Gartner, H. Kreye, R. Kirchheim, *Mater. Sci. Eng. A* 353 (2003) 74–79.
- [17] T. Al-Kassab, H. Wollenberger, G. Schmitz, R. Kirchheim, in: M. Rühle, F. Ernst (Eds.), *High Resolution Imaging and Spectrometry of Materials*, Springer-Verlag, Berlin, 2003, pp. 271–320.
- [18] G. Hibbard, U. Erb, K.T. Aust, G. Palumbo, *Mater. Res. Soc. Symp. Proc.* 580 (2000) 183–188.
- [19] M. Abraham, P. Holdway, A. Cerezo, G.D.W. Smith, *Mater. Sci. Forum* 386–388 (2002) 397–402.
- [20] A.A. Rasmussen, A. Gholinia, P.W. Trimby, M.A.J. Somers, *Mater. Sci. Forum* 467–470 (2004) 1345–1350.
- [21] F. Czerwinski, J.A. Szpunar, *Nanostruct. Mater.* 11 (1999) 669–676.
- [22] F. Czerwinski, H. Li, M. Megret, J.A. Szpunar, *Mater. Res. Soc. Symp. Proc.* 451 (1997) 501–504.
- [23] Y.B. Park, S.-H. Hong, C.S. Ha, H.Y. Lee, T.H. Yim, *Mater. Sci. Forum* 408–412 (2002) 931–936.
- [24] Y.B. Park, J. Park, C.S. Ha, T.H. Yim, *Mater. Sci. Forum* 408–412 (2002) 919–924.
- [25] H. Li, F. Czerwinski, J.A. Szpunar, *Nanostruct. Mater.* 9 (1997) 673–676.